Cation−π Interaction in the Polyolefin Cyclization Cascade Uncovered by Incorporating Unnatural Amino Acids into the Catalytic Sites of Squalene Cyclase

Noriko Morikubo,[†] Yoriyuki Fukuda,[†] Kazumasa Ohtake,[§] Naoko Shinya,[‡]
Daisuke Kiga,[‡,#] Kensaku Sakamoto,[‡] Miwako Asanuma,[‡] Hiroshi Hirota,[‡,||]
Shigeyuki Yokoyama,[‡,§,⊥] and Tsutomu Hoshino*,[†]

*Contribution from the Department of Applied Biological Chemistry, Faculty of Agriculture, and
Graduate School of Science and Technology, Niigata University, Ikarashi 2 no-cho, 8050,
Niigata, Niigata 950-2181, Japan, RIKEN Genomic Sciences Center, 1-7-22 Suehiro-cho,
Tsurumi-ku, Yokohama, 230-0045, Japan, Department of Biophysics and Biochemistry, Graduate
School of Science, The University of Tokyo, 7-3-1 Hongo, Bunkyo-ku, Tokyo 113-0033, Japan,
International Graduate School of Arts and Sciences, Yokohama City University,
1-7-29 Suehiro-cho, Tsurumi-ku, Yokohama 230-0045, Japan, and RIKEN SPring-8 Center,
Harima Institute, 1-1-1 Kouto, Sayo, Hyogo 679-5148, Japan*

Received May 15, 2006; E-mail: hoshitsu@agr.niigata-u.ac.jp

Abstract: It has been assumed that the π-electrons of aromatic residues in the catalytic sites of triterpene cyclases stabilize the cationic intermediates formed during the polycyclization cascade of squalene or oxidosqualene, but no definitive experimental evidence has been given. To validate this cation−π interaction, natural and unnatural aromatic amino acids were site-specifically incorporated into squalene−hopene cyclase (SHC) from *Alicyclobacillus acidocaldarius* and the kinetic data of the mutants were compared with that of the wild-type SHC. The catalytic sites of Phe365 and Phe605 were substituted with *O*-methyltyrosine, tyrosine, and tryptophan, which have higher cation−π binding energies than phenylalanine. These replacements actually increased the SHC activity at low temperature, but decreased the activity at high temperature, as compared with the wild-type SHC. This decreased activity is due to the disorganization of the protein architecture caused by the introduction of the amino acids more bulky than phenylalanine. Then, mono-, di-, and trifluorophenylalanines were incorporated at positions 365 and 605; these amino acids reduce cation−π binding energies but have van der Waals radii similar to that of phenylalanine. The activities of the SHC variants with fluorophenylalanines were found to be inversely proportional to the number of the fluorine atoms on the aromatic ring and clearly correlated with the cation−π binding energies of the ring moiety. No serious structural alteration was observed for these variants even at high temperature. These results unambiguously show that the π-electron density of residues 365 and 605 has a crucial role for the efficient polycyclization reaction by SHC. This is the first report to demonstrate experimentally the involvement of cation−π interaction in triterpene biosynthesis.

1. Introduction

Triterpenes are abundant in nature and confer important biological functions. The polycyclic triterpene, including the steroid scaffold, is biosynthesized via ring-forming reactions (polycyclization) of the linear molecule of squalene or 2,3-oxidosqualene having a chain length C_{30}.[1] The structural diversity is remarkable, and ca. 120 kinds of triterpene skeletons have been found until now; lanosterol from vertebrates and fungi, cycloartenol and α-, β-amyrin from plants, and hopene from prokaryote are well-known. The polycyclization reactions proceed with complete regio- and stereospecificity, leading to the formation of new C−C bonds and chiral centers (Scheme 1); seven chiral centers and four C−C bonds for lanostane skeleton, while nine stereocenters and five C−C bonds for hopanoid. Scheme 1 shows the cyclization mechanism of (3*S*)-2,3-oxidosqualene **1** to form lanosterol **2** (A) and that of squalene **4** to afford pentacyclic hopene **5** and hopanol **6** (B). The question of how the structural diversity and multistep reactions are attained by a single cyclase enzyme has attracted prominent organic and biological chemists for over a half-century.[2−5] Prokaryotic squalene-hopene cyclase (SHC) is of

---

[†] Niigata University.
[‡] RIKEN Genomic Sciences Center.
[§] The University of Tokyo.
[||] Yokohama City University.
[⊥] RIKEN SPring-8 Center, Harima Institute.
[#] Current address: Interdisciplinary Graduate School of Science and Engineering, Tokyo Institute of Technology, 4259 Nagatsuta, Midori-ku, Yokohama 226-0026, Japan.

(1) For recent reviews, see: (a) Yoder, R. A.; Johnston, J. N. *Chem. Rev.* **2005**, *105*, 4730−4756. (b) Segura, M. J. R.; Jackson, B. E.; Matsuda, S. P. T. *Nat. Prod. Rep.* **2003**, *20*, 304−317. (c) Hoshino, T.; Sato, T. *Chem. Commun.* **2002**, 291−301. (d) Wend, K. U.; Schulz, G. E.; Corey, E. J.; Liu, D. R. *Angew. Chem., Int. Ed.* **2000**, *39*, 2812−2833.
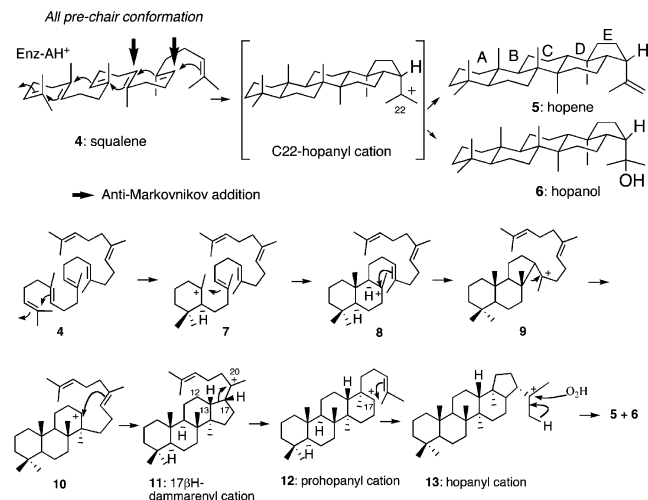
(2) Woodward, R. B.; Bloch, K. *J. Am. Chem. Soc.* **1953**, *75*, 2023−2024.

Scheme 1. Polycyclization Mechanism of 2,3-oxidosqualene **1** by Eukaryotic Lanosterol Synthase (A) and that of Squalene **4** by Prokaryotic Hopene Synthase (B)*a*

(A) Oxidosqualene-Lanosterol Cyclase

pre-chair-boat-chair conformation

(B) Squalene-Hopene Cyclase

All pre-chair conformation
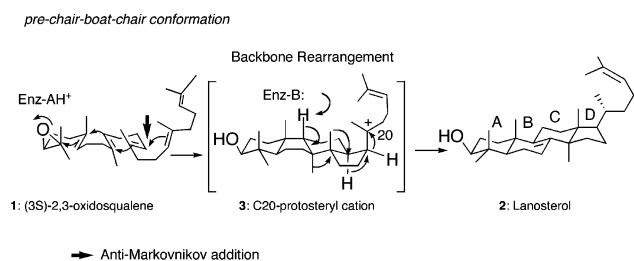
a Transient carbocation intermediates are generated during the sequential ring-forming reactions. In the polycyclization process, anti-Markovnikov addition occurs as shown by the bold arrows (➞); one point is found for lanosterol construction, while two points for hopene biosynthesis. To tolerate the violation of Markovnikov rule found in the polycyclization reaction, two concepts have been proposed. One is that the discrete carbocations are involved in the cyclization reactions and the stable tertiary captions **9** and **11** are first generated according to Markovnikov rule, and then the ring expansion process from five- to six-membered ring occurs as shown in the reactions of **9** ➞ **10** and **11** ➞ **12**. In contrast, the alternative is that the polycyclization reaction proceeds with a concertedness, whereby anti-Markovnikov addition is attained by proper folding of squalene **4** with aid of the cyclase enzyme in the reaction cavity.[13] It has been proposed that the residue Phe365 stabilizes the bicyclic cation **8**,[9d] while Phe605 stabilizes the 6,6,6,5-fused tetracyclic **11** and the 6/6/6/6-fused tetracyclic cation **12**.[9h]

particular note from the aspect of molecular evolution, because it is believed that eukaryotic cyclases evolved from the prokaryotic SHC.[6] The polycyclization mechanism of acyclic squalene is analogous to that of eukaryotic oxidosqualene cyclase (OSC), although OSC involves further intricate backbone rearrangement reactions accompanying 1,2-shifts of hy-

dride and methyl groups (Scheme 1). Recently, we have shown that the substrate specificity of prokaryotic cyclase can be successfully altered into that of eukaryotic type, which are specific to (3*S*)-2,3-oxidosqualene.[7] Since the three-dimensional X-ray crystallographic structure of squalene cyclase has been elucidated by Schulz and co-workers in 1997,[8] there have been remarkable advances on the catalytic mechanism by SHC,[1c] which have been disclosed mainly by the site-directed mutagenesis experiments.[9] Site-directed mutations led to the early truncation of the polycyclization cascade[9] and/or to the aberrant cyclization products whose stereochemistry is opposite to that of the normal cyclization intermediates, strongly indicating that the stereochemical destiny during the polycyclization cascade is directed by the steric bulk size of the active-site residues.[9g] Functional analyses of many site-directed mutants and the identification of the enzymic products from substrate analogues[10] demonstrated that the reaction cavity is compact and all the folded pre-chair conformation is firmly constricted by the cyclase; thus, no flexible motion of the folded conformation is allowed inside the reaction cavity once the polycyclization has started.[10d,f] Transient carbocation intermediates, e.g., **3** and **7**−**13** are presumed to be involved in the polycyclization cascade (Scheme 1).[1c] Previously, it was suggested that the carboxylate anion of acidic amino acid residues likely works as the cation-stabilizing groups.[11] In contrast, Dougherty proposed that interaction between the intermediate carbocations and π-electrons of aromatic amino acids (cation−π interaction) is responsible for the polycyclization reactions.[12] Indeed, the X-ray crystal structure revealed that the reaction cavity is lined with aromatic amino acid residues.[8] The aromatic residues would be more preferable than the carboxylate anion as the role for stabilizing cationic intermediates, because the carboxylate anion in the

(3) Conforth, J. W.; Conforth, R. H.; Donninger, C.; Popjack, G.; Shimizu, Y.; Ichii, S.; Forchielli, E.; Capsi, E. *J. Am. Chem. Soc.* **1965**, *87*, 3224−3228.

(4) (a) Eschenmoser, A.; Ruzicka, Jerger, O.; Arigoni, D. *Helv. Chim. Acta* **1955**, *38*, 1890−1904. (b) Eschenmoser, A.; Arigoni, D. *Helv. Chim. Acta* **2005**, *88*, 3011−3050.

(5) (a) Corey, E. J.; Ortiz de Montellano, P. R. *J. Am. Chem. Soc.* **1967**, *86*, 3362−3363. (b) Corey, E. J.; Virgil, S. C.; Sarshar, S. *J. Am. Chem. Soc.* **1991**, *113*, 8171−8172. (c) Corey, E. J.; Virgil, S. C.; Cheng, H.; Baker, C. H.; Matsuda, S. P. T.; Singh, V.; Sarshar, S. *J. Am. Chem. Soc.* **1995**, *117*, 11819−11820. (d) Corey, E. J.; Cheng, H. *Tetrahedron Lett.* **1996**, *37*, 2709−2712.

(6) (a) Rohmer, M.; Bouvier, P.; Ourisson, G. *Proc. Natl. Acad. Sci. U.S.A.* **1979**, *76*, 847−851. (b) Ourisson, G.; Rohmer, M.; Poralla, K. *Annu. Rev. Microbiol.* **1987**, *41*, 301−333. (c) Ourisson, G. *Pure Appl. Chem.* **1989**, *61*, 345−348.

(7) Hoshino, T.; Shimizu, K.; Sato, T. *Angew. Chem., Int. Ed.* **2004**, *43*, 6700−6703.

(8) (a) Wendt, K. U.; Lenhart, A.; Schulz, G. E. *Science* **1997**, *277*, 1811−1815. (b) Wendt, K. U.; Poralla, K.; Schulz, G. E. *J. Mol. Biol.* **1999**, *286*, 175−187. (c) Reinert, D. J.; Balliano, G.; Schulz, G. E. *Chem. Biol.* **2004**, *11*, 121−126.

(9) Our studies, see: (a) Sato, T.; Kanai, Y.; Hoshino, T. *Biosci. Biotechnol. Biochem.* **1998**, *62*, 407−411. (b) Sato, T.; Abe, T.; Hoshino, T. *Chem. Commun.* **1998**, 2617−2618. (c) Sato, T.; Hoshino, T. *Biosci. Biotechnol. Biochem.* **1999**, *63*, 1171−1180. (d) Hoshino, T.; Sato, T. *Chem. Commun.* **1999**, 2005−2006. (e) Hoshino, T.; Kouda, M.; Abe, T.; Ohashi, S. *Biosci. Biotechnol. Biochem.* **1999**, *63*, 2038−2041. (f) Sato, T.; Hoshino, T. *Biosci. Biotechnol. Biochem.* **1999**, *63*, 2189−2198. (g) Hoshino, T.; Abe, T.; Kouda, M. *Chem. Commun.* **2000**, 441−442. (h) Hoshino, T.; Kouda, M.; Abe, T.; Sato, T. *Chem. Commun.* **2000**, 1485−1486. (i) Sato, T.; Hoshino, T. *Biosci. Biotechnol. Biochem.* **2001**, *65*, 2233−2242. (j) Sato, T.; Sasahara, S.; Yamakami, T.; Hoshino, T. *Biosci. Biotechnol. Biochem.* **2002**, *66*, 1660−1670. (k) Sato, T.; Kouda, M.; Hoshino, T. *Biosci. Biotechnol. Biochem.* **2004**, *68*, 728−738. Poralla and co-worker's studies, see: (l) Full, C.; Poralla, K. *FEMS Microbiol. Lett.* **2000**, *183*, 221−224. (m) Ochs, D.; Kaletta, C.; Entian, K. D.; Beck-Sickinger, A.; Poralla, K. *J. Bacteriol.* **1992**, *174*, 298−302. (n) Schmitz, S.; Füll, C.; Glaser, T.; Albert, K.; Poralla, K. *Tetrahedron Lett.* **2001**, *42*, 883−885. (o) Merkofer, T.; Pale-Grosdemange, C.; Wendt, K. U.; Rohmer, M.; Poralla, K. *Tetrahedron Lett.* **1999**, *40*, 2121−2124. (p) Pale-Grosdemange, C.; Merkofer, T.; Rohmer, M.; Poralla, K. *Tetrahedron Lett.* **1999**, *40*, 6009−6012.

(10) (a) Hoshino, T.; Kondo, T. *Chem. Commun.* **1999**, 731−732. (b) Hoshino, T.; Ohashi, S. *Org. Lett.* **2002**, *25*, 2553−6. (c) Hoshino, T.; Nakano, S.; Kondo, T.; Sato, T.; Miyoshi, A. *Org. Biomol. Chem.* **2004**, *2*, 1456−1470. (d) Nakano, S.; Ohashi, S.; Hoshino, T. *Org. Biomol. Chem.* **2004**, *2*, 2012−2022. (e) Hoshino, T.; Kumai, Y.; Kudo, I.; Nakano, S.; Ohashi, S. *Org. Biomol. Chem.* **2004**, *2*, 2650−2657. (f) Abe, T.; Hoshino, T. *Org. Biomol. Chem.* **2005**, *3*, 3127−3139. (g) Abe, I.; Tanaka, H.; Noguchi, H. *J. Am. Chem. Soc.* **2002**, *124*, 14514−14515. (h) Tanaka, H.; Noguchi, H.; Abe, I. *Org. Lett.* **2004**, *5*, 803−806. (i) Tanaka, H.; Noguchi, H.; Abe, I. *Tetrahedron Lett.* **2004**, *45*, 3093−3096. (j) Tanaka, H.; Noguchi, H.; Abe, I. *Org. Lett.* **2005**, *7*, 5873−5876.

(11) (a) Johnson, W. S.; Telfer, S. J.; Cheng, S.; Schubert, U. *J. Am. Chem. Soc.* **1987**, *109*, 2517−2518. (b) Johnson, W. S.; Lindell, S. D.; Steele, J. *J. Am. Chem. Soc.* **1987**, *109*, 5852−5853.

(12) (a) Dougherty, D. A. *Science* **1996**, *271*, 163−168. (b) Zacharias, N.; Dougherty, D. A. *Trends Pharmacol. Sci.* **2002**, *23*, 281−287.

cyclases is likely to form the covalent bonding with the cationic intermediates, but this irreversible bond formation is unlikely in case of hydrophobic aromatic residues.

To evaluate the cation−π interaction, we previously prepared the SHC mutants with Tyr or Trp in place of Phe365 or Phe605.[9d,h] These have been assumed to be essential residue for catalysis;[1c,d,8b,c] it has been proposed that Phe365 stabilizes the 6,6-fused bicyclic cation **8**,[9d] while Phe605 does the 6,6,6,5-fused tetracyclic **11** and the 6/6/6/6-fused tetracyclic cation **12**,[9h] based on the product profiles afforded by the Phe365Ala and the Phe605Ala mutants.[9d,h] The replacement by Tyr or Trp was expected to enhance the reaction rate due to an increased π-electron density as compared with Phe. However, the specific activities of the mutants against incubation temperatures showed an unusual profile significantly differing from a typical bell-shape; accelerated reaction rate was observed at low incubation temperature region, but decreased velocity at high-temperature region when compared with those of the wild-type. We could not get the exact answer of why the abnormal profile was found for the Tyr and Trp mutants. Thus we have failed to give clear experimental evidence for the cation−π interaction, although the enhanced reaction rates observed at lower temperatures may suggest the augmented cation−π interaction.[9d,h] Further study had been required to establish the cation−π interaction in triterpene biosynthesis. Two contradictory mechanisms have been proposed for the ring-propagation reaction; one is a stepwise mechanism via discrete carbocations as shown in Scheme 1, which involves the ring enlargement process from the five- to six-membered ring (**9** → **10** and **11** → **12**), the five-membered ring being initially formed according to venerable Markovnikov rule; on the other hand, the alternative is the concerted mechanism[13,14] that the cascade takes place without the involvement of discrete cationic intermediates and without the violation of Markovnikov rule, by holding the substrate in the proper conformation to effect the cascade in the active groove of the protein.[13] This debate for the two inconsistent ideas is still ongoing.

To provide a deep insight into the polycyclization mechanism, we planned to incorporate unnatural aromatic amino acids into squalene cyclase site-specifically. The introduction of unnatural amino acid(s) at specific position(s) provides a powerful tool for analyzing protein function.[15] In the present study, *O*-methyltyrosine (*OMe*Tyr) and fluorophenylalanines (FluoroPhes) were incorporated into SHC in place of Phe365 and Phe605, and the resulting mutants were examined for the catalytic activity. The aromatic π-electron density of *OMe*Tyr is greater than that of Phe, and therefore an increased reaction rate is expected for the variant with *OMe*Tyr. On the other hand, a fluorine atom has an extremely higher electronegativity but a

(13) (a) Hess, B. A., Jr. *J. Am. Chem. Soc.* **2002**, *124*, 10286−10287. (b) Hess, B. A., Jr. *Org. Lett.* **2003**, *5*, 165−167. (c) Hess, B. A., Jr.; Smentek, L. *Org. Lett.* **2004**, *6*, 1717−1720. (d) Hess B. A., Jr. *Collect. Czech. Chem. Commun.* **2004**, *69*, 261−266. (e) Hess B. A., Jr. *Eur. J. Org. Chem.* **2004**, 2239−2242.
(14) (a) Rajamani, R.; Gao, J. *J. Am. Chem. Soc.* **2003**, *125*, 12768−12781. (b) Gao, D.; Pan, Y.-K.; Buyn, K.; Gao, J. *J. Am. Chem. Soc.* **1998**, *120*, 10286−10287.
(15) (a) Wang, L.; Brock, A.; Herberich, B.; Schultz, P. G. *Science* **2001**, *292*, 498−500. (b) Chin, J. W.; Santoro, S. W.; Martin, A. B.; King, D. S.; Wang, L.; Schultz, P. G. *J. Am. Chem. Soc.* **2002**, *124*, 9026−9027. (c) Mehl, R. A.; Anderson, J. C.; Santoro, S. W.; Wang, L.; Martin, A. B.; King, D. S.; Horn, D. M.; Schultz, P. G. *J. Am. Chem. Soc.* **2003**, *125*, 935−939. (d) Wang, L.; Schultz, P. G. *Chem. Commun.* **2002**, 1−10. (e) Wang, L.; Xie, J.; Schultz, P. G. *Annu. Rev. Biophys. Biomol. Struct.* **2006**, *35*, 225−249.

supressor tRNA	+	+	+	+	+	+
*OMe*TyRS	-	-	+	+	+	+
OMeTyr	+	+	-	-	+	+

←80kDa
←SHC
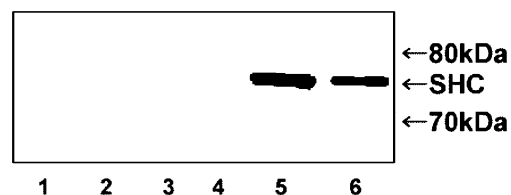←70kDa

1   2   3   4   5   6

Figure 1. Western blot analysis of the incorporation of *OMe*Tyr at position 605 (lanes 1, 3, and 5) or at position 365 (lanes 2, 4, and 6) of SHC under the indicated conditions. The SHC variants with *OMe*Tyr were detected by an anti-His-tag antibody.

similar van der Waals radius compared to that of a hydrogen atom. Thus, substitution with FluoroPhe is anticipated to inhibit the cation−π interaction without causing a structural alteration of the cyclase enzyme, possibly leading to a slower reaction rate with a normal bell-shape profile. We constructed three variants with FluoroPhe, which have one to three fluorine atoms on Phe benzene ring, based on the idea that the greater number of fluorine atoms leads to the slower reaction rate. The decreased specific activities and the formation of the prematurely cyclized products with five-membered ring, which were caused by the decreased π-electron density of the FluoroPhe variants, verified that cation−π interaction plays a crucial role both for the efficient annulation reaction and for the ring enlargement process in triterpene biosynthesis.

2. Results and Discussion

2.1. Site-Specific Incorporation of Unnatural Amino Acids. To prepare several milligrams of SHC variants with *OMe*Tyr and those with FluoroPhes, we employed cell-based and cell-free systems, respectively. The *Escherichia coli* system for the site-specific incorporation of *OMe*Tyr, developed by Schultz and co-workers,[15a] involves this unnatural amino acid supplemented in the growth media and a pair of an engineered tyrosyl-tRNA synthetase (*OMe*TyrRS) and an amber suppressor tRNA from *Methanococcus jannaschii*. *OMe*TyrRS specifically recognizes *OMe*Tyr and the suppressor tRNA to produce *O*-methyltyrosyl suppressor tRNA, which in turn translates amber codons into *OMe*Tyr. *OMe*TyrRS does not recognize the other amino acids or endogenous tRNA species in *E. coli*, while neither of *OMe*Tyr and the suppressor tRNA is recognized by the other aminoacyl-tRNA synthetases than *OMe*TyrRS.

Introduction of an SHC gene with an amber codon at position 365 or 605 into this *E. coli* system led to the production of the SHC variant with *OMe*Tyr at the amber position. To prevent misincorporation of any of the 20 common amino acids at the amber position, we used *E. coli* strain BL21(DE3), which has no endogenous activity of amber suppression. Since the efficiency of the suppression is less than 100%, the SHC molecules truncated at the amber position were produced. A His-tag was added at the C-terminus of SHC to be separated from the truncated molecules. Figure 1 shows the western blot analyses of the SHC variants (Phe365*OMe*Tyr and Phe605-*OMe*Tyr) expressed in the *E. coli* cells. Only in the presence of all of *OMe*Tyr, *OMe*TyrRS, and suppressor tRNA, the full-length SHC was produced, which indicated that *OMe*Tyr was site-specifically incorporated at position 365 or 605.
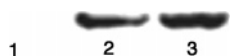
Figure 2. Western blot analysis of the expressed SHC variants in the cell-free system. The SHC variants were detected by an anti-His-tag antibody. (Lane 1) Suppressor tRNA[Phe] added to the translation reaction was not charged with any amino acid. (Lane 2) SHC variant gene with the Phe605Amber and Tyr606Ala mutations were expressed under the addition of FluoroPhe-charged suppressor tRNAPhe. (Lane 3) Expression of the SHC (Tyr606Ala).

SHC variants with 4-fluoro-L-phenylalanine (F_1−Phe), 3,4-difluoro-L-phenylalanine (F_2−Phe), and 3,4,5-trifluoro-L-phenylalanine (F_3−Phe) at position 365 or 605 were produced in a cell-free translation system, because no cell-based system is available for the site-specific incorporation of the fluoro-amino acids. We used a cell-free translation system based on an S30 extract from *E. coli* BL21(DE3) cells. Before SHC synthesis, an amber suppressor tRNA derived from *E. coli* tRNA[Phe] was charged with FluoroPhes by *E. coli* phenylalanyl-tRNA synthetase (PheRS) in the presence of elongation factor Tu (EF-Tu) in a test tube. PheRS, which can recognize both of FluoroPhe and phenylalanine, attaches only FluoroPhe to the suppressor tRNA in the absence of phenylalanine. In addition, the aminoacylation of the suppressor tRNA[Phe], which has a low activity,[16] requires the enzyme of such a high concentration that can be achieved only in vitro. The added EF-Tu protects the ester bond formed between FluoroPhe and tRNA from hydrolysis. The charged suppressor tRNA was then applied to the cell-free translation of an SHC gene with an amber codon. The efficiency of amino acid incorporation in response to amber codons is generally higher with purine base A or G at the 3′ side of the amber codon than pyrimidine base C or U.[17] Therefore, as for the SHC variant with FluoroPhes at position 605, the tyrosine codon, UAC, at position 606 were substituted with alanine codon, GCG; the Tyr606Ala substitution has no influence on the kinetics of squalene cyclization by SHC.[9i] The subjection of uncharged suppressor tRNA[Phe] led to no production of the full length of SHC (Figure 2), indicating that the suppressor tRNA was not charged in the cell-free translation system. Only FluoroPhes therefore occupied the amber position of the full-length SHCs. This cell-free system yielded 0.1 mg/mL of the SHC variants with FluoroPhes.

2.2. MS Analyses of SHCs Substituted with Unnatural Amino Acids. To confirm the incorporation of *OMe*Tyr or FluoroPhe in response to UAG codon accurately, the purified SHCs were digested with trypsin (limited digestion) and the fragment mixtures were then subjected to LC/MS measurement (ESI-Q/TOF). Figure 3A shows the LC/MS data of the Tyr606Ala mutated SHC and 3B shows the proteins into which F_1−Phe was incorporated at position 605 of the Y606A mutated SHC (the double mutated SHC, Phe605F_1−Phe/Tyr606Ala). The LC/MS showed *m/z* 1403.03 $(M + 3H)^{3+}$, triply charged ion, which corresponds to the fragment covering the peptide residues Gly577-Arg613 of the Tyr606Ala mutated SHC (Calcd: 4205.91, Obsd: 4206.07 as the monoisotopic mass of the peptide residues). In contrast, the FluoroPhe-incorporated SHC exhibited *m/z* 1408.97 $(M + 3H)^{3+}$, i.e., Calcd: 4223.90, Obsd: 4223.89 as the monoisotopic mass, verifying that one fluorine atom was incorporated. Introduction of F_2−Phe into
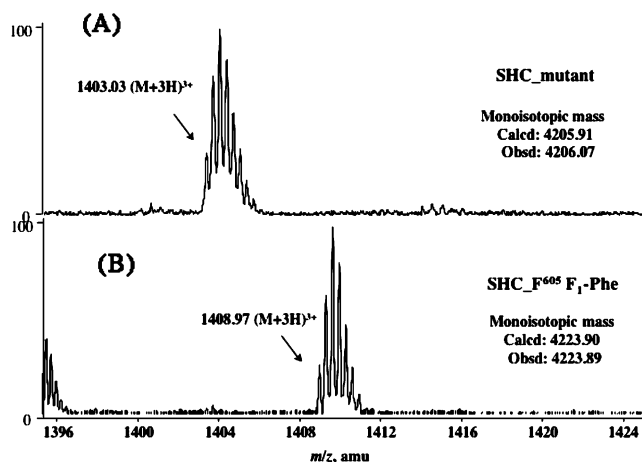
(16) Peterson, E. T.; Uhlenbeck, O. C. *Biochemistry* **1992**, *31*, 10380−10389.
(17) Phillips-Jones, M. K.; Watson, F. J.; Martin, R. *J. Mol. Biol.* **1993**, *233*, 1−6.

Figure 3. ESI-Q/TOF mass spectra. (A) Tyr606Ala mutated SHC. (B) double mutant of Phe605F_1−Phe/Tyr606Ala, in which 4-fluorophenylalanine (F_1−Phe) was further incorporated into the Tyr606Ala. The increased mass of *m/z* 18 verified that a fluorine atom was incorporated.

position 605 was also confirmed by observing the corresponding mass increase (see Supporting Information). The incorporation of *OMe*Tyr at position 605 was also demonstrated; *m/z* 1433.69 $(M + 3H)^{3+}$ was observed for the wild-type SHC and *m/z* 1443.71 $(M + 3H)^{3+}$ for the *OMe*Tyr-incorporated SHC, these MS data showing the molecular weights of the peptide fragments to be 4298.04 Da (Calcd: 4297.94) and 4328.11 Da (Calcd: 4327.95), respectively (Supporting Information). Incorporation of the unnatural amino acids at position 365 was also demonstrated by observing the peptide fragment mass covering the residues Arg355-Arg389 (Supporting Information). These MS data coupled with the SDS-PAGE analyses (Figures 1 and 2) conclusively show that the unnatural amino acids are being incorporated with high fidelity and high selectivity.

2.3. Kinetic Analyses of Tyr-, OMeTyr-, and Trp-Incorporated SHCs with Higher π-Electron Density. Figure 4 (solid lines) shows the specific activities of SHCs mutated at position 605 vs incubation temperatures. The catalytic optimal temperature of the wild-type SHC was found at 55 °C accompanying a typical bell-shaped curve. The SHC used in this experiment is from *Alicyclobacillus acidocaldarius*, a thermoacidophilic bacterium, thus showing the high optimum temperature (55 °C) for the catalysis.[9] If cation−π interaction occurs during the polyene cyclization reaction, the reaction rates of all the mutants should be increased at the entire temperature range due to the enhanced π-electron density. However, all the mutants had lower activity at high temperature region, but higher activity at low temperatures, compared to the wild-type, thus leading to lower optimal temperatures (Figure 4, solid lines). An unusual profile differing from a normal bell-shape of the wild-type was found, especially in the case of the Phe605Trp and Phe605*OMe*Tyr mutants; three distinctive phases were observed: at 30−40 °C, the activities were increased; at 40−50 °C, a steady state was reached; at 55−70 °C, the activities decreased (Figure 4, solid lines). The enhanced reaction rates at low-temperature region (<40 °C) implicate the occurrence of cation−π interaction, but why did the reaction rate significantly decrease at higher temperatures? The kinetic data were estimated according to Lineweaver−Burk equation (Table 1). The K_m values of all the mutants, which were estimated at both 40 and 50 °C, were significantly larger than that of the wild-type, indicating that the affinity between the mutants and the
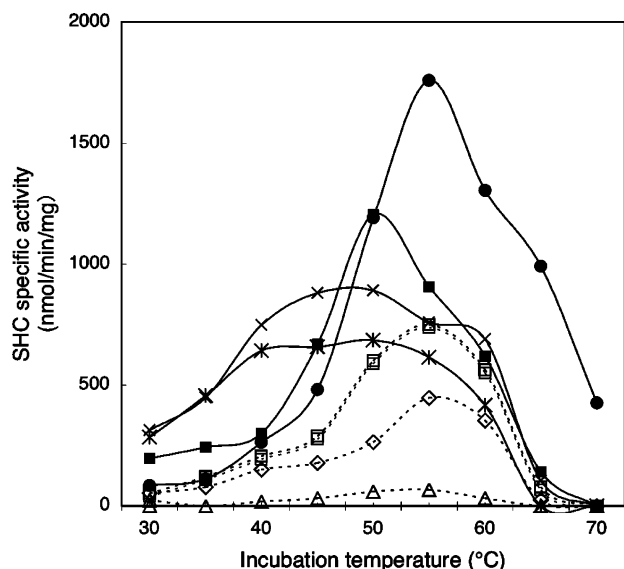
Figure 4. Specific activities of the wild-type and the mutated SHCs having *OMe*Tyr, Tyr, Trp, 4-monofluoroPhe (F_1−Phe), 3,4-difluoroPhe (F_2−Phe), and 3,4,5-trifluoroPhe (F_3−Phe) at position 605. Solid lines: the wild-type and the Phe606Ala mutant (●); Phe605Tyr mutant (■); Phe605Trp mutant (×); Phe605*OMe*Tyr mutant (*). Dotted lines: FluoroPhe mutants, in which Tyr606 are further mutated to Ala. The specific activity of the Tyr606Ala is the same as the wild type (see the text and ref 9i). F_1−Phe mutant (□); F_2−Phe mutant (◇); F_3−Phe mutant (△). The kinetic data of the double mutants correspond to those of the single mutant with FluoroPhes at position 605, because the kinetic values of the wild-type are the same as those of the site-directed Tyr606Ala mutant.

Table 1. Kinetic Parameters of the Site-Directed Mutants Measured at 40 °C and at 50 °C, Which Were Determined by Estimating the Amount of Hopene **5** Produced in the Enzymic Reactions

	measured at 40°C		measured at 50 °C	
	K_m (μM)	k_{cat} (min^{-1})	K_m (μM)	k_{cat} (min^{-1})
wild-type	15.4	15	24.2	119
Phe605Tyr	52.5	16	104	109
Phe605*OMe*Tyr	105	27	152	42.0
Phe605Trp	118	55	191	79.0
Phe365Tyr	nd[a]	nd	130	10.2
Phe365*OMe*Tyr	nd	nd	185	8.95
Phe365Trp	nd	nd	—[b]	—

[a] nd: not measured. [b] —: not determined due to marginal activity.

substrate markedly decreased in the following order: Phe (the wild-type) > Tyr > *OMe*Tyr > Trp; the smallest K_m for the wild-type, with the largest one for the Trp mutant. The more bulky substituents gave the larger K_m (looser binding) (Table 1) with elevating incubation temperatures, which would have resulted in the profile of steady state (at 40−50 °C), despite π-electron density having been enhanced. Figure 5 shows the circular dichroism (CD) of the wild-type and the mutants, which were measured at 50 °C. The intensities of the negative Cotton effect were in the following order: Phe (the wild-type) > Tyr > *OMe*Tyr > Trp. The decreased Cotton effect found in the mutants suggests the disorganization of the protein architecture. The difference of Cotton effect (Δ molecular ellipticities) between the wild-type and the mutants was greatly enhanced by elevating temperatures in the following order: Trp $\geq$ *OMe*Tyr > Tyr (Figure 6), which is in a good accordance with the increasing order of K_m values (Table 1). Thus, it is strongly indicated that the decreased activities at higher temperatures
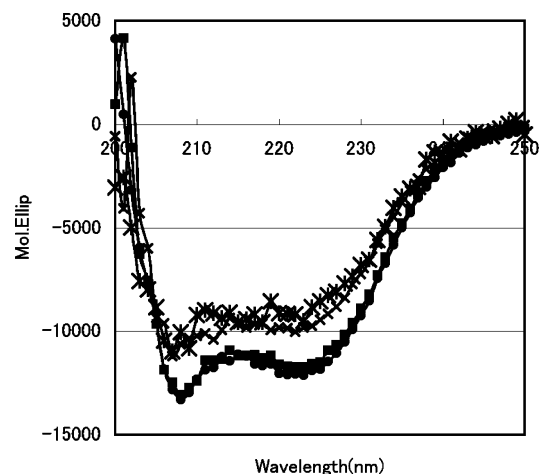
Figure 5. CD spectra of the mutated SHCs measured at 50 °C. This figure shows that the protein architectures of Phe605*OMe*Tyr and Phe605Trp mutants were noticeably altered at the catalytic optimal temperature of 50 °C (see the solid lines of Figure 4). (●) wild-type, (■) Phe605Tyr, (×) Phe605Trp, (*) Phe605*OMe*Tyr. At ambient temperature, the CD spectra of the three mutants were superimposable on that of the wild-typ.[9d,h] However, significant local change of the enzyme had indeed occurred by the introduction of the larger steric bulk sizes, despite no visible effect on the overall CD having been found at ambient temperature.
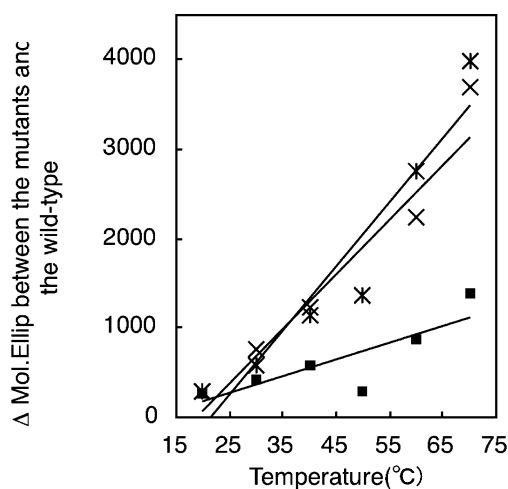

Figure 6. CD intensities (molecular ellipticities, Δ mol ellip.) of the mutated SHCs subtracted from that of the wild-type, which were plotted at 222 nm against temperatures. The transparent solutions of the Trp and OMeTyr mutated SHCs became cloudy at 75 °C, indicating the occurrence of thermal denaturation. (■) Phe605Tyr mutant; (*) Phe605*OMe*Tyr mutant; (×) Phe605Trp mutant. The slopes of the Phe605Trp and Phe605*OMe*Tyr mutants were significantly larger than that of the Phe605Tyr mutant, indicating that the enzyme structures of the Phe605Trp and Phe605*OMe*Tyr mutants were more markedly disordered than that of the Phe605Tyr, due to the replacement of the increased steric bulk sizes.

(Figure 4) would have resulted from thermal denaturation of the cyclase structure; the Trp mutant with the largest steric bulk size underwent the highest susceptibility to high temperatures among all the mutants. Thus, the wild-type with Phe (the smallest size) at position 605 showed the highest stability against thermal denaturation. These results indicate that the geometrical local change of SHC protein architecture had been induced even by single amino acid substitution. However, it is noticeable that the reaction velocities of the Trp, *OMe*Tyr and Tyr mutants were enhanced at lower temperature region (30−45 °C) (Table 1 and Figure 4, solid lines) despite the affinity having been looser due to the introduction of larger amino acid, thus implying
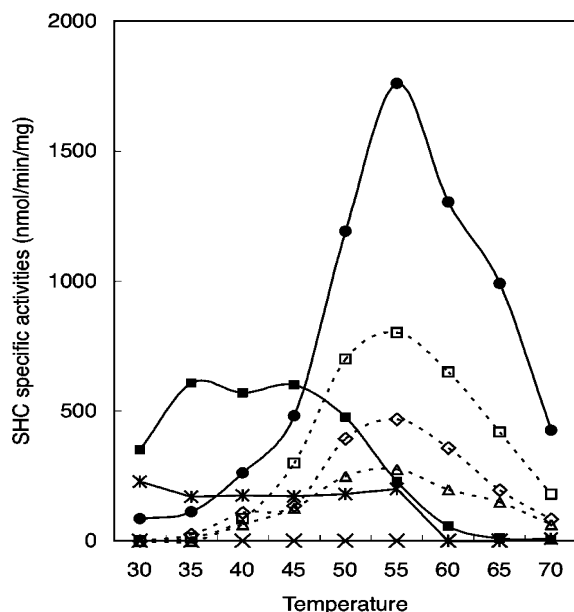
Figure 7. Specific activities of the mutated SHCs into which natural and unnatural amino acids were incorporated at position 365. Wild-type (●); Phe365Tyr (■); Phe365Trp (×); Phe365*OMe*Tyr (*); Phe365F$_1$–Phe (□) Phe365F$_2$–Phe (◇); Phe365F$_3$–Phe (△).

that cation–π interaction is likely during squalene cyclization reaction.

Figure 7 (solid lines) depicts the specific activities of the SHCs having electron-donating substituents at position 365. The Phe365 residue has been suggested to stabilize the 6/6-fused bicyclic tertiary cation **8** through cation–π interaction.[8b,9d] These mutants also showed abnormal profiles in a way similar as the SHC variants mutated at position 605 (see the solid lines of Figures 4 and 7). As in case of the mutants at position 605, the more bulky substituents gave the larger K_m (Table 1), leading to the profile of steady state (30−55 °C for the Phe365*OMe*Tyr and 35−45 °C for the Phe365Tyr). Despite the indole ring having richest π-electron density among the aromatic rings used, the Phe365Trp mutant had no enzymatic activity (Figure 7); however, the Phe605Trp had still somewhat high activity (Figure 4). This suggests that a local change of the protein structure at position 365 occurred more significantly, compared to that at position 605 (Table 1 and compare Figure 4 with 7); thus, the active-site region at position 365 is more tightly compact than that at position 605.

2.4. Kinetic Analyses of Fluorophenylalanine-Incorporated SHCs with Lowered π-Electron Density. Figures 4 and 7 (doted lines) show the specific activities of the Phe605FluoroPhes/ Tyr606Ala and Phe365FluoroPhe mutants against incubation temperatures, respectively. The profiles showed a typical bell-shape similar to that of the wild-type. As we have reported previously, no difference of the kinetic data (K_m and k_{cat}) and CD was found between the Tyr606Ala and the wild-type SHCs.[9i] Thus, the kinetic data of the double mutants at positions 605 and 606 correspond to those of the single mutant with FluoroPhes at position 605. The optimal temperatures (55 °C) of all the FluoroPhe mutants at positions 365 and 605 for the catalysis were the same as that of the wild-type and no difference of the CD spectra between all of the fluorine-inserted SHCs and the wild-type SHC was found at temperature range of 20− 70 °C (see Supporting Information). Thus, the steric effect

Table 2. Kinetic Values of the FluoroPhe-Incorporated SHCs Measured at 50 °C[a]

	K_m (μM)	k_{cat} (min^{-1})	k_{cat}/K_m (min^{-1}/μM)	relative activity (%)
wild-type or Tyr606Ala mutant	24.2	119	4.92	100
Phe605F$_1$-Phe/Tyr606Ala	27.9	49.2	1.76	35.8
Phe605F$_2$-Phe/Tyr606Ala	32.4	32.2	0.99	20.2
Phe605F$_3$-Phe/Tyr606Ala	–	–	–	–
Phe365F$_1$-Phe	35.2	65.1	1.85	37.6
Phe365F$_2$-Phe	41.6	55.2	1.33	27.0
Phe365F$_3$-Phe	47.9	45.1	0.94	19.1

[a] All the SHCs into which the FluoroPhes are incorporated at position 605 are double mutants, in which Tyr606 is further replaced by Ala in order to enhance the expression level of the unnatural FluoroPhe-incorporated SHCs (see section 2.1 in the text). Kinetic values of the wild-type are the same as those of the site-directed Tyr606Ala mutant, which was clearly demonstrated in our previous experiments.[9i] Thus, the kinetic data of the double mutants correspond to those of the single mutant with FluoroPhes at position 605. All the FluoroPhe-incorporated SHCs at position 365 are the single amino acid substituted mutants, but not doubly mutated ones. The K_m and k_{cat} values of Phe605F$_3$−Phe were not determined due to the negligibly small activity.

caused by the incorporation of the FluoroPhes on the enzyme structure was minimum. Indeed, in the case of the FluoroPhe mutants at position 605, the changes in the K_m's by increasing the number of fluorine atoms were modest (Table 2): 1.15-fold and 1.34-fold looser binding for the F$_1$−Phe and for the F$_2$−Phe mutants, respectively, as compared with that of the wild-type. On the contrary, the k_{cat}'s were more significantly decreased; 2.4-fold slower for the F$_1$−Phe variant and 3.7-fold reduction for the F$_2$−Phe mutant compared to that of the wild-type. In other words, with increasing the number of substituted fluorine atoms, the more decreased reaction rates were clearly observed, but the binding remained almost unchanged, highly indicating that Figure 4 (dotted lines) displays essentially the effect of π-electron density on the enzyme activity; thus, the occurrence of cation–π interaction at position 605 was unambiguously demonstrated. Daugherty and co-workers calculated the cation–π binding energies for the binding of the sodium cation lying over the center of the aromatic rings.[18] The plots of the specific activities against the binding energies had a good correlation (Figure 8, correlation $R^2 = 0.96$ for the FluoroPhe mutants at position 605), further supporting that the Phe605 residue actually plays the critical role for cation–π interaction. On the other hand, the Phe365FluoroPhe variants had the more increased K_m values compared to those of the Phe605FluoroPhe mutants (Table 2): 1.45-fold, 1.72-fold, and 1.98-fold poorer binding for the F$_1$−Phe, the F$_2$−Phe, and the F$_3$−Phe variants, respectively, compared to that of the wild-type, but the k_{cat}s were significantly decreased with increasing the number of the fluorine atoms (1.83-fold, 2.16- and 2.64-fold decreased for the F$_1$−, F$_2$−, and F$_3$−Phe variants, respectively). The more increased K_m values of the FluoroPhe variants at position 365, compared to those at position 605, indicate that the active site region around position 365 is more tightly packed than that of position 605. This is consistent with the inference from the comparison of the Tyr, *OMe*Tyr, and Trp variants at positions 365 with those at position 605, which was discussed in the previous section. No change in K_m and a significantly lowered k_{cat} by the fluorination are ideal for verifying cation–π

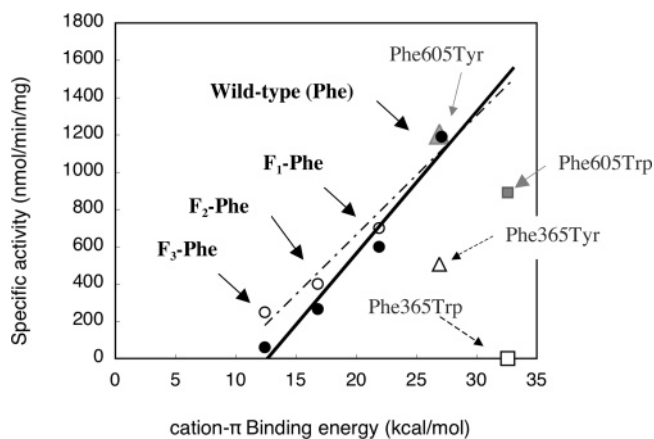(18) Mecozzi, S.; West, A. P., Jr.; Daugherty, D. A. *Proc. Natl. Acad. Sci. U.S.A.* **1996**, *93*, 10566−10571.

Figure 8. Relationship between the specific activities of FluoroPhe-inserted SHCs and cation−π binding energies. Cation−π binding energies (kcal/mol) of Phe, F_1−Phe, F_2−Phe and F_3−Phe are reported to be 27.1, 21.9, 16.8, and 12.4, respectively.[18] The SHC activities were determined by estimating the amount of hopene produced at 50 °C for 60 min. Closed circles and solid line: the mutated SHCs into which FluoroPhes and Ala were incorporated at both positions 605 and 606, respectively, but the activities correspond to that of the single mutant at position 605 (see text). Open circles and dotted line: the FluoroPhe variants mutagenized only at position 365. The correlations for the site-directed mutants with Trp and Tyr at positions 365 and 605 were added to clearly show that the Trp and the Tyr mutants at position 365 greatly shifted from the straight line. The cation−π binding energies for Trp and Tyr were reported to be 32.6 and 26.9 kcal/mol, respectively,[18] the value for *OMe*Tyr having not been calculated.

interaction. Due to occurrences of somewhat larger changes in both k_{cat}'s and K_m's for the FluoroPhe variants, it may be difficult to strongly indicate cation−π interaction at position 365. However, it should be noted that the increased K_m values by incorporating the F_1− to F_3−Phe at position 365 (K_m = 35−48) were significantly smaller, compared to those by introducing the Tyr and *OMe*Tyr (K_m = 130−180, and an exceptionally large K_m for the Trp mutant) (see Tables 1 and 2), thus, leading to the same catalytic optimal temperature of the F_1− to F_3−Phe variants as that of the wild-type (Figure 7, dotted lines), which permitted us to compare the relative activities k_{cat}/K_m between the FluoroPhe mutants and the wild-type at a given temperature. The relative activities were inversely proportional to the number of the attached fluorine atoms (Table 2). Furthermore, the specific activities of the FluoroPhe-incorporated mutants at position 365 were well correlated with cation−π binding energies (Figure 8, R^2 = 0.95). This good correlation also would have been obtained due to the relatively small changes, though not to be neglected, in the K_m's of the FluoroPhe variants at position 365. In contrast, the Trp and the Tyr mutants at position 365 having the exceptionally large K_m values greatly shifted from the straight line of the cation−π binding energies (Figure 8). Thus, it would be highly probable that Phe365 also has a role in stabilizing transient carbocation intermediate as well as Phe605, for which cation−π interaction was credibly established as described above.

2.5. Product Profiles by the SHC Variants with Fluorophenylalanines. Figure 9 shows the GC traces of hexane extract from the incubation mixture of squalene **4** with the Phe605F_2−Phe mutated SHC. In the case of the wild-type, the GC peaks other than hopene **5** and hopanol **6** was marginal,[19] but the mutant with the FluoroPhe afforded two new peaks of **14** and **15** in significantly large amounts besides **5** and **6**. Products **14** and **15** were identified to be 20(R)-13(17)-

dammarene and 20(R)-(17αH)-12(13)-dammarene, respectively, by comparing the GC/MS with those of the authentic samples, which were previously isolated by us from some mutants.[9g,h] Production of **14** and **15** having a 6/6/6/5-fused tetracycle was also found in the incubation mixtures of squalene **4** with F_1− and F_3−Phe mutants. Formation mechanism of **14** and **15** is illustrated in Scheme 2. The tetracyclic dammarenyl cations **16** could be produced according to Markovnikov rule. To gain the 20(R)-stereochemistry, the dammarenyl skeleton must have 17α-H and 17β-side chain as shown in **16**,[10c,20] indicating that squalene **4** was folded in a chair/chair/chair/boat conformation **18**. In contrast, chair/chair/chair/chair conformation **17** leads to 20(S)-dammarenyl skeleton.[10c,20] The hydride shift of H-17 to C20-cation and the deprotonation of H-13 on **16** in anti-periplanar manner could give **14**. The 1,2-hydride shifts of H-17 and H-13 in an anti-parallel fashion, followed by the deprotonation of H-12ax, could afford **15**. The π-electron density is significantly decreased by the introduction of fluorine atom on Phe, but the size of F_2−Phe is almost the same as that of Phe, which was demonstrated indeed by the kinetic and CD results as described above. Formation of the tetracyclic ring system by Markovnikov closure definitively demonstrates that the π-electron density of Phe605 is important for the five- to six-membered ring enlargement process to yield **12** from **11**. In fact, the production amounts of **14** and **15** relative to **1** was markedly increased with increasing the number of fluorine atoms; the ratio of the sum of **14** and **15** to **1** was 0.09, 0.17, and 0.94 by introducing F_1, F_2, and F_3, respectively. Cation **16** is preferred to cation **11**, because unfavorable steric repulsion (1,3-diaxial interaction) occurs among 30-Me, 21-Me, and 27-Me for all-chair conformation **17**, but the repulsive interaction is less in chair/chair/chair/boat conformation **18**.[10c] The preference of **16** to **11** is further supported by the computational energy calculation.[21a] Failure to form the unstable secondary cation **12**, which was caused by the decreased π-electron density, would have led to the energetically favored **16** during the cyclization reaction. Thus, the aromatic Phe is crucial not only for stabilizing the intermediary secondary cation **12**, but also for posing the energetically unfavorable conformation **17**. No truncated cyclization product was found in the incubation mixtures with the Tyr, *OMe*Phe, and Trp mutants, further indicating that the energetically favored chair/chair/chair/boat conformation **18** was generated due to the reduction in π-electron density.

Previously, we reported that the Phe365Ala mutant afforded the premature cyclization products having the 6/6-fused bicyclic skeleton (polypodatetraene and neopolypodatetraene),[9d,i] which could be produced from intermediary cation **8**. However, no detectable amount of these bicyclic compounds was found in the incubation mixtures with the FluoroPhe variants (Figure 9C). A geometrical local change would have occurred around position 365, due to the replacement of a significantly decreased steric bulk size of Ala, possibly leading to the termination of the polycyclization reaction at bicyclic intermediate stage **8**. No detectable amount of the bicyclic products by the FluoroPhe variants further indicates that the structural alteration of the

(19) Pale-Grosdemange, C.; Feil, C.; Rohmer, M.; Poralla, K. *Angew. Chem., Int. Ed.* **1998**, *37*, 2237−2240.
(20) Abe, I.; Rohmer, M. *J. Chem. Soc., Perkin Trans. 1* **1994**, *30*, 783−791.
(21) (a) Xiong, Q.; Rocco, F.; Wilson, W. K.; Xu, R.; Ceruti, M.; Matsuda, S. P. T. *J. Org. Chem.* **2005**, *70*, 5362−5375. (b) Matsuda, S. P. T.; Wilson, W. K.; Xiong, Q. *Org. Biomol. Chem.* **2006**, *4*, 530−543.
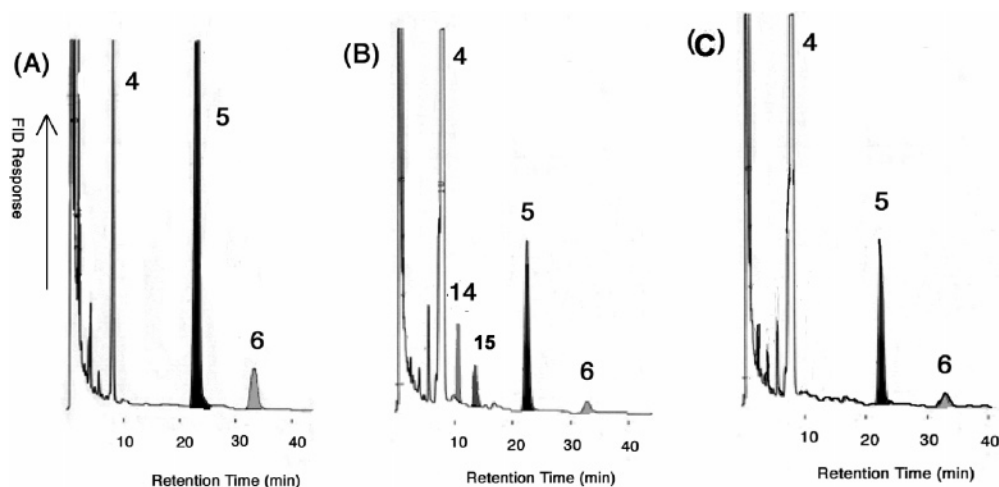
Figure 9. GC traces of hexane extracts from the incubation mixtures of squalene **4** with the wild-type SHC (A), with the mutated SHC having F_2–Phe at position 605 (B) and with the mutant having the F_2–Phe at position 365 (C). Incubation conditions: squalene substrate 1.0 mg, SHCs 100 μg, pH 6.0 and 55 °C for 3 h. An excess of Triton X-100 used in the incubations was removed by a short SiO_2 column, eluting with a mixture of hexane and EtOAc (100:20). Peaks 4, 5, and 6 correspond to squalene, hopene, and hopanol, respectively. Peaks 14 and 15 were identified as 20(R)-13(17)-dammarene and 20(R)-(17αH)-12(13)-dammarene, respectively.

Scheme 2. Formation Mechanism of **14** and **15** by the Phe605F_2-Phe Mutated SHC
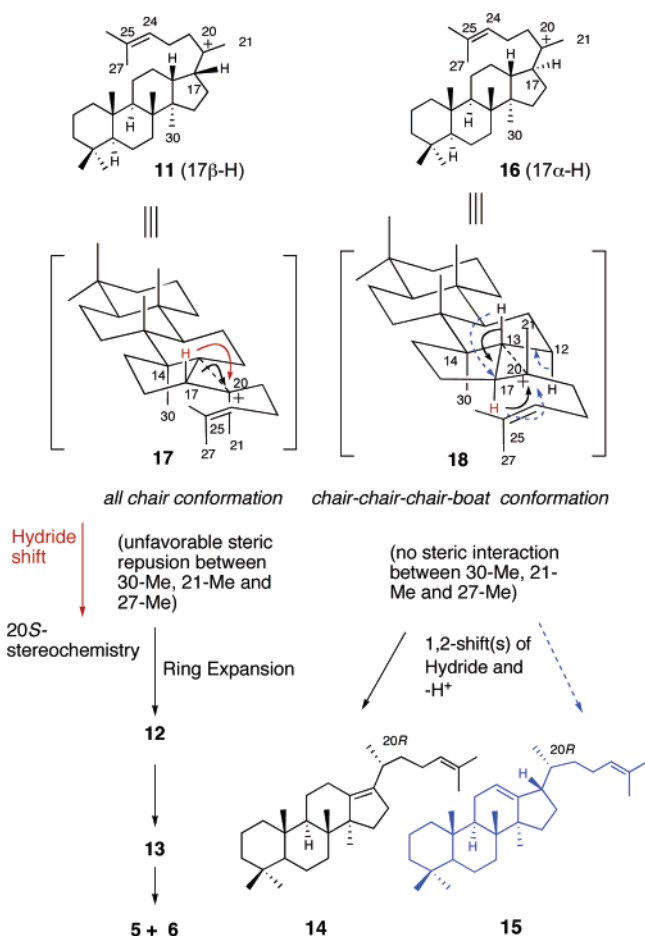
FluoroPhe-incorporated SHCs was a little. Now many definitive evidences are available that alteration of the steric bulk size of active sites affords the aberrant cyclization product(s).[1c,9g,22]

3. Concluding Remarks

We described here the first site-specific incorporation of unnatural amino acids into a triterpene cyclase. The magnitude

of the cation–π interaction depends on the nature of the aromatic amino acids involved in protein. Of the natural aromatic residues, Trp forms the strongest interaction with cations due to the greater electron density of Trp relative to Tyr or Phe. However, the Trp- and *OMe*Tyr-incorporated SHCs showed significantly decreased CD magnitude with elevating temperatures and led to a lowered catalytic optimal temperature, compared to the wild-type. In this study, we showed that introduction of the larger substituents at the active site led to a looser binding to the substrate and that the reaction rate was more dramatically decreased at elevated temperatures due to enhanced susceptibility of the mutants to thermal denaturation, compared to that of the wild-type. On the other hand, the difference between the steric bulk size of FluoroPhe and that of Phe is marginal, but the π-electron density of the FluoroPhe is significantly lower than that of Phe. In fact, this study showed that, in the case of the FluoroPhe variants at position 605, the increase in K_m was small (1.15-fold for the F_1–Phe mutant), but the reduction in k_{cat} was more significant (2.42-fold for the F_1–Phe mutant), compared to those of the wild-type, and the catalytic optimal temperature was identical to that of the wild-type. In addition, the enzyme activities of the SHC variants with FluoroPhes were found to be inversely proportional to the number of the fluorine atoms on the aromatic ring, and clearly correlated with cation–π binding energies of the aromatic ring moiety (Figure 8). These findings definitively established that the residue Phe605 stabilizes carbocation intermediates via cation–π interaction. On the other hand, the Phe365FluoroPhe mutants had relatively larger K_m's, as compared with those of the Phe605FluoroPhe variants, and also had significantly decreased k_{cat}. The more increased K_m's indicate the severely tight packing around position 365. No change in K_m and a significant lowering in k_{cat} for the FluoroPhe mutants are ideal

(22) (a) Joubert, B. M.; Hua, L.; Matsuda, S. P. T. *Org. Lett.* **2000**, *2*, 339–341. (b) Segura, M. J. R.; Meyer, M. M.; Matsuda, S. P. T. *Org. Lett.* **2000**, *2*, 2257–2259. (c) Meyer, M. M.; Segura, M. J. R.; Wilson, W. K.; Matsuda, S. P. T. *Angew. Chem., Int. Ed.* **2000**, *39*, 4090–4092. (d) Meyer, M. M.; Xu, R.; Matsuda, S. P. T. *Org. Lett.* **2002**, *4*, 1395–1398. (e) Segura, M. J. R.; Lodeiro, S.; Meyer, M. M.; Patel, A. J.; Matsuda, S. P. T. *Org. Lett.* **2002**, *4*, 4459–4462. (f) Lodeiro S.; Segura M. J.; Stahl, M.; Schulz-Gasch, T.; Matsuda, S. P. T. *ChemBioChem* **2004**, *5*, 1581–1585. (g) Wu, T. K.; Chang, C. H. *ChemBioChem* **2004**, *5*, 1712–1715.

for proposing cation−π interaction. Thus, the enhanced K_m's of the FluoroPhe variants at position 365 may not give convincing evidence for cation−π interaction at position 365. However, the increased K_m values were significantly smaller compared to those of the Trp, OMeTyr, and Tyr mutants, leading to little effect on the catalytic optimum temperature (Figure 7, dotted line) and to a good correlation between the enzyme activity and cation−π binding energies (Figure 8, dotted line). Furthermore, the relative activities (k_{cat}/K_m) of the FluoroPhe variants were decreased progressively with increasing the number of fluorine atoms (Table 2). Therefore, it is fair to assume that the Phe365 residue does stabilize an intermediary cation through cation−π interaction. In addition, the crystal structure of human lanosterol synthase also revealed that the Phe444 residue, equivalent to Phe365 of SHC, stabilizes the tertiary cations at C6 and C10 through cation−π interaction.[23] The van der Waals radius of the hydrogen atom (120 pm) is closest to that of fluorine atom (147 pm). The increased radius (27 pm), the difference between fluorine and hydrogen, for the fluorine-inserted mutant is significantly small, but squalene cyclase differentiated fluorine from hydrogen to some extent, especially with respect to the site 365. The difference of the van der Waals radius (152 pm, extra oxygen atom attached on Phe) between the Tyr mutant and the wild-type (Phe), is relatively larger, which caused thermal denaturation of the protein (Figure 7). Thus, the present study affords the additional evidence that the enzyme cavity of the cyclase is exceptionally compact; thus, no flexible motion of squalene molecule **4** is allowed inside the reaction cavity. The tightly packed enzyme cavity would enforce squalene **4** into a meandering conformation, which was shown by the X-ray crystallographic analysis;[8c] the folded conformation allows the close contact of a double bond to carbocation intermediate to facilitate the subsequent ring-forming reaction. Cation−π interaction in conjunction with the meandering conformation of the substrate would effectively foster the progressive propagation of carbocyclic rings.

It is of particular note that the aromatic π-electrons of Phe can facilitate the ring enlargement process from five- to six-membered D-ring (from tertiary to secondary cations), as evidenced by the formation of 6/6/6/5-fused tetracycles **14** and **15** by the Phe605FluoroPhe variants. Corey et al. gave the experimental evidence that the six-membered C-ring in lanosterol skeleton is produced by the ring expansion process from five-membered C-ring, which was initially formed according to Markovnikov rule.[5c,d] The ring expansion process has been supported also by biomimetic studies.[24] Incubation of 22,23-dihydro-2,3-oxidosqualene, lacking a terminal double bond, with β-amyrin synthase gave bacchar-12-en-3β-ol via 6/6/6/6-cation.[25] This finding indicates that the D-ring expansion did occur without the benefit of cation stabilization by a terminal double bond of the side chain; thus, the anchimeric assistance by an approach of double bond to intermediate cations would

be modest, which was also suggested by Matsuda et al.[21b] (3S,-22S)-2,3:22,23-Dioxidosqualene was converted to 17,24-epoxy-25-hydroxybaccharane-3β,25-diol by lupeol synthase,[26] further supporting the involvement of secondary baccharenyl cation. In addition, secondary cation **12** with 6/6/6/6-fused tetracycle was trapped also by incubating squalene **4** with Ile261Gly and Ile261Ala mutated SHCs,[9g] in which the crucial catalytic site of Phe605 was still retained. Thus, the ring expansion would occur with aid of a greater interaction between the secondary cation intermediate and π-electrons of the catalytic sites. Previously, Jensen and Jorgensen suggested, on the basis of the force-field calculation, that the energy barrier between secondary and tertiary cations might be lowered by selective placement of nucleophilic group from the protein backbone or side chain including the indole ring of tryptophan.[27] The present study clearly validated this idea. In conclusion, this study unambiguously demonstrated that cation−π interaction occupies a key position in the catalytic mechanisms by triterpene cyclases.

Cation−π interactions are now well recognized to play an important role in biological systems, including protein structure,[28] protein−ligand interactions,[29] ion channels,[30] etc. Carbocationic intermediates are assumed to be involved in many key enzymes of isoprenoid biosyntheses,[30] as exemplified by isopentenyldiphosphate isomerase,[31,32] prenyltransferase, [31,33] squalene synthase[31,34] and many terpene cyclases.[31] The cation−π interaction proposed for these isoprenoid biosyntheses has been inferred from the X-ray crystallography and/or mutagenesis using conventional natural amino acids. To establish the cation−π interactions for the terpenoid biosyntheses at enzymatic level, the site-specific incorporation experiments of unnatural amino acids using in vivo and/or in vitro translation systems would be necessary, because variation of steric and electronic environments using 20 natural amino acids is limited, that is, a number of insights that would have been impossible using conventional site-directed mutations would be gained. The technology of the site-specific incorporation of unnatural amino acids into protein is fascinating tool for the correct understanding enzyme mechanisms.

(23) Thoma, R.; Schulz-Gasch, T.; D'Arcy, B.; Benz, J.; Aebi, J.; Dehmlow, H.; Hennig, M.; Stihle, M.; Ruf, A. *Nature* **2004**, *432*, 118−1222.
(24) For examples: (a) van Tamelen, E. E.; Willet, J.; Schwartz, M.; Nadeau, R. *J. Am. Chem. Soc.* **1966**, *88*, 5937−5938. (b) van Tamelen, E. E. *J. Am. Chem. Soc.* **1982**, *104*, 6480−6481. (c) Nishizawa, M.; Takenaka, H.; Hayashi, Y. *J. Am. Chem. Soc.* **1985**, *107*, 522−523. (d) Nishizawa, M.; Yadav, A.; Imagawa, H.; Sugihara, T. *Tetrahedron Lett.* **2003**, *44*, 3867−3870. (e) Nishizawa, M.; Yadav, A.; Iwamoto, Y.; Imagawa, H. *Tetrahedron* **2004**, *60*, 9223−9234.
(25) Abe, I.; Sakano, Y.; Tanaka, H., Lou, W.; Noguchi, H.; Shibuya, M.; Ebizuka, Y. *J. Am. Chem. Soc.* **2004**, *126*, 3426−3427.
(26) Shan, H.; Segura, M. J. R.; Wilson, W. K.; Lodeiro, S.; Matsuda, S. P. T. *J. Am. Chem. Soc.* **2005**, *127*, 18008−18009.
(27) Jenson, C.; Jorgensen, W. L. *J. Am. Chem. Soc.* **1997**, *119*, 10846−10854.
(28) (a) Fernandez-Recio, J.; Romero, A.; Sancho, J. *J. Mol. Biol.* **1999**, *290*, 319−330. (b) Ting, A. Y.; Shin, I.; Lucero, C.; Schultz, G. *J. Am. Chem. Soc.* **1998**, *120*, 7135−7136. (c) Loewenthal, R.; Sancho, J.; Fersht, A. R. *J. Mol. Biol.* **1992**, *224*, 759−770. (d) Burley, S. K.; Petsko, G. A. *FEBS Lett.* **1986**, *203*, 139−143. (e) Perutz, M. F.; Fermi, G.; Abraham, D. J.; Poyart, C.; Bursaux, E. *J. Am. Chem. Soc.* **1986**, *108*, 1064−1078.
(29) (a) Susman, J. L.; Harel, M.; Folow, F.; Oefner, C.; Goldman, A.; Toker, L.; Silman, I. *Science* **1991**, *253*, 872−879. (b) Zhong, W.; Gallivan, J. P.; Zhang, Y.; Li, L.; Lester, H. A.; Dougherty, D. A. *Proc. Natl. Acad. Sci. U.S.A.* **1998**, *95*, 12088−12093. (c) Satow, Y.; Cohen, G. H.; Padlan, E. A.; Davis, D. R. *J. Mol. Biol.* **1986**, *190*, 593−604. (d) Beene, D. L.; Brandt, G. S.; Zhong, W.; Zacharias, N. M.; Lester, H. A.; Dougherty, D. A. *Biochemistry* **2002**, *41*, 10262−10269. (e) Lummis, S. C. L.; Beene, D.; Harrison, N. J.; Lester, H. A.; Dougherty, D. A. *Chem. Biol.* **2005**, *12*, 993−997.
(30) (a) Okada, A.; Miura, T.; Takeuchi, H. *Biochemistry* **2001**, *40*, 6053−6060. (b) Kumpf, R. A.; Dougherty, D. A. *Science* **1993**, *261*, 1708−1710.
(31) Cane, D. E.; Barton, D., Nakanishi, K., Meth-Cohn, O., Eds. Isoprenoids Including Carotenoids and Steroids. In *Comprehensive Natural Product Chemistry*, 2nd ed.; Pergamon/Elsevier: Amsterdam, 1999.
(32) Durbecq, V.; Sainz, G.; Oudjama, Y.; Clantin, B.; Bompard-Gilles, C.; Tricot, C.; Caillet, J.; Stalon, V.; Droogmans, L.; Villere, V. *EMBO J.* **2001**, *20*, 1530−1537.
(33) Ogura, K.; Koyama, T. *Chem. Rev.* **1998**, *98*, 1263−1276.
(34) (a) Tansey, T. R.; Shechter, I. *Biochim. Biophys. Acta* **2000**, *1529*, 49−62. (b) Pandit, J.; Danley, D. E.; Schulte, G. K.; Mazzalupo, S.; Pauly, T. A.; Hayward, C. M.; Hamanaka, E.; Thompson, J. F.; Harwood, H. J., Jr. *J. Biol. Chem.* **2000**, *275*, 30610−30617.

Methods and Materials

Incorporation of *OMe*Tyr into SHC Protein in *E. coli*. The gene coding for *OMe*TyrRS was generated from the wild-type TyrRS gene from *M. jannaschii* to contain the substitutions of Tyr^{32}→Gln^{32}, Glu^{107}→Thr^{107}, Asp^{158}→Ala^{158}, and Leu^{162}→Pro^{162}. These substitutions allow OMeTyrRS to recognize *OMe*Tyr specifically.[15a] In addition, the substitution of Asp^{286}→Tyr^{86} was introduced to enhance the recognition of suppressor tRNA.[35] The used suppressor tRNA was derived from *M. jannaschii* tRNA^{Tyr}, containing the base substitutions of C17A, U17aG, U20C, G34C, G37A, and U47G. The G34C substitution makes the tRNA to recognize amber codon, and the others prevent misacylation of this tRNA by the endogenous aminoacyl-tRNA synthetases from *E. coli*.[15a] The genes for *OMe*TyrRS and the suppressor tRNA were cloned in the pACYC184 vector (NEB) to create plasmid pLMR-o, where the enzyme and tRNA were expressed from the *trpS* and *lpp* promoters, respectively.

The phenylalanine codons at positions 365 and 605 of the SHC gene were mutagenized to be amber codon (UAG) by using the QuickChange site-directed mutagenesis kit (Stratagene, La Jolla, CA, U.S.A.) to create SHC (Am365) and SHC (Am605). These mutant genes were cloned in the expression vector pET26b (Novagene), where a His$_6$ tag was added to the C-terminus of SHC to facilitate protein purification by Ni^{2+} affinity column chromatography. Ocher codon (UAA) was used to stop the translation of SHC. *E. coli* BL21(DE3) cells were transformed with both of pET26b carrying the SHC mutant gene and pLMR-o, and were then cultured in the LB medium containing kanamycin of 50 µg/mL and chloramphenicol of 25 µg/mL together with 1 mM *OMe*Tyr. The harvested cells were subjected to ultrasonication on ice in a buffer containing 50 mM NaH$_2$PO$_4$, 300 mM NaCl, and 10 mM imidazole. The obtained extracts were subjected to centrifugation at 10000*g* for 20 min. The resultant supernatants were loaded onto a Ni agarose column (Qiagen) equilibrated with a buffer (50 mM NaH$_2$PO$_4$, 300 mM NaCl, 10 mM imidazole, 1% Triton X-104). The SHC with the His tag was eluted with 250 mM imidazole including 1% Triton X-104. The protein concentration was determined by the Bio-Rad protein assay kit by using a standard curve for bovine serum albumin.

Incorporation of FluoroPhes into SHC in a Cell-Free Protein Synthesis. To enhance the expression in a cell-free system based on an S30 extract of *E. coli* BL21(DE3) cells, silent mutations, suggested by the ProteoExpert software (Roche), were introduced into the 5′-terminal sequence of the SHC gene. The sequence of the first 36 bases of this gene was thus changed to: ATGGCAGAACAACTTGTA-GAAGCGCCGGCCTACGCG (the silent mutations are underlined). The substitution of tyrosine codon with alanine codon at position 606 was performed for SHC (Am605) by using the QuickChange site-directed mutagenesis kit (Stratagene, La Jolla, CA) to create SHC (Am605 Ala606). For expression in the cell-free protein synthesis system, the SHC mutant genes, SHC (Am365) and SHC (Am605 Ala606), were cloned in the pIVEX2.3d vector (Roche), where the His tag was added at the C-terminus of SHC.

The *E. coli pheS* and *pheT* genes encoding phenylalanyl-tRNA synthetase (PheRS) were cloned between the *Sma*I and *Bam*HI sites of the pUC119 vector (Takara). PheRS was overproduced from this plasmid in *E. coli* cells, and was purified by successive chromatography on the columns of DEAE-Toyopearl and Toyopearl phenyl-650M (Tosoh, Tokyo) using a linear gradient of 50–250 mM KCl and that of 800–0 mM (NH$_4$)$_2$SO$_4$, respectively.

The gene coding *E. coli* suppressor tRNA^{Phe}, with the sequence of GGCCGGATAGCTCAGTCGGTAGAGCAGGGGATTCTAAAT-CCCCGTGTCCTTGGTTCGATTCCGAGTCCGGCCACCA, was transcribed by the method of in vitro transcription using T7 RNA

polymerase.[36] Preparation of EF-Tu was according to the published protocol.[37] To convert EF-Tu from the GDP form to the GTP form, 0.15 µM EF-Tu was incubated with 600 µM GTP in a buffer (50 mM Tris-HCl at pH7.5, 50 mM MgCl$_2$, 150 mM NH$_4$Cl) on ice for 30 min. The suppressor tRNA^{Phe} (40 µM), 2 mM ATP, 0.5 mM FluoroPhe, and PheRS (1 µM) were added to this mixture of EF-Tu and GTP, and aminoacylation reaction was then performed at 37 °C for 30min. The reaction mixture was finally subjected to phenol extraction, and the charged tRNA was then precipitated by ethanol and dissolved in water.

The synthesis of SHC variants was performed at 30 °C for 7 h in a coupled transcription/translation cell-free system with dialysis.[38] The internal reaction mixture (9 mL) consisted of 58 mM Hepes−KOH buffer (pH 7.5), containing 1.2 mM ATP, 0.8 mM each of GTP, CTP, and UTP, 1.7 mM DTT, 0.64 mM 3′,5′-cyclic AMP, 200 mM potassium glutamate, 27.5 mM ammonium acetate, 10.7 mM magnesium acetate, 80 mM creatine phosphate, 250 µg/mL creatine kinase, 500 µM of each of the 20 amino acids, 4.0% PEG8000, 25 mM phosphoenolpyru-vate, 35 µg/mL *L*-(−)-5-formyl-5,6,7,8-tetrahydrofolic acid, 0.05% sodium azide, a tRNA mixture (170 µg/mL), the pIVEX2.3d-SHC plasmid (4 µg/mL) as the template, S30 extract (2.7 mL), T7 RNA polymerase (66.6 µg/mL), and the charged suppressor tRNA^{Phe} (0.01µM). The external solution (90 mL) contained all of the components of the internal solution except for creatine kinase, tRNA, the template plasmid, T7 RNA polymerase, and S30 extract. The dialysis membrane, MWCO 50,000 Spectra/Por, was from Spectrum. Purification of the tagged SHC variants was performed as described above.

SDS-PAGE and Western Blot Analysis. Proteins, separated on a 10% SDS-polyacrylamide gel, were analyzed by western blot. Mouse anti-His-tag monoclonal antibody was used as the primary antibody, and the goat anti-mouse IgG conjugated with HRP were used as the secondary antibody. Detection was performed by the ECL plus immunodetection system (Novagene) after treatment with the antibodies. The band intensity was measured using an image analyzer, LAS-1000 plus (Fuji Photo Film, Tokyo).

MS Analyses of SHCs Substituted with Unnatural Amino Acids. Tryptic digestions were performed using standard procedures. For example, 2 µL (0.2 µg) of 0.1 mg/mL trypsin solution was added to a solution of SHC protein (∼10 µg or 130−140 pmol) in a sodium citrate buffer, and 100 mM sodium hydrogen carbonate was also added to reach a final concentration of 20 mM. The mixture was kept at 37 °C for overnight. When the protein was available as in gel, in-gel tryptic digestion was applied.

A QSTAR mass spectrometer (Applied Biosystems, U.S.A.) equipped with an Agilent 1100 series LC system (Agilent Technologies, U.S.A.) was used for LC/MS analyses. LC conditions were as follows: LC column: Mightysil RP-18 GP 50-1.0 (3 µm) (Kanto Chemical Co., Inc., Japan); flow rate: 5 µL/min; mobile phase A: water and B: acetonitrile with 0.1% formic acid; gradient: 5−60% B in 80 min). Electrospray was applied for the ionization and the objective peptide fragments were obtained from the mass chromatography.

Incubation Conditions for the Determination of Kinetic Data. A mixed solution, which was composed of 0.5 mM squalene, 0.2% Triton X-100, and 50 µg of the homogeneously purified enzyme in a sodium citrate buffer (60 mM, pH 6.0), was prepared in a final volume of 5 mL for the enzyme reactions. Incubation was carried out for 60 min at different temperatures (30, 35, 40, 45, 50, 55, 60, 65, or 70 °C) to examine the thermal stability of the cyclases. To determine the kinetic parameters, the incubation was conducted for 60 min at 40 or 50 °C (Tables 1 and 2). To terminate the reaction, 15% methanolic KOH (6 mL) was added. The lipophilic enzymatic products (**5** and **6**) and starting

(35) Kobayashi T.; Nureki O.; Ishitani R.; Yaremchuk A.; Tukalo M.; Cusack S.; Sakamoto K.; Yokoyama S. *Nat. Struct. Biol.* **2003**, *10*, 425−432.

(36) Milligan, J. F.; Uhlenbeck, O. C. *Methods Enzymol.* **1989**, *180*, 51−62.
(37) Sakamoto, K.; Ishimaru, S.; Kobayashi, T.; Walker, J. R.; Yokoyama, S. *J. Bacteriol.* **2004**, *186*, 5899−5905.
(38) Kigawa, T.; Yabuki, T.; Yoshida, Y.; Tsutsui, M.; Ito, Y.; Shibata, T.; Yokoyama, S. *FEBS Lett.* **1999**, *442*, 15−19.

material **4**, which remained unchanged, were extracted four times with hexane (5 mL) from the incubation mixtures, and the amount of **5** thus produced was evaluated by a Shimadzu GC-8A instrument equipped with a DB-1 capillary column (0.53 mm × 30 m). Kinetic parameters K_m and k_{cat} were determined according to the Lineweaver−Burk equation. GC/MS spectra were obtained with a JEOL SX 100 mass spectrometer.

Circular Dichroism of SHCs. SHCs have been usually purified and assayed in a sodium citrate buffer (pH 6.0) containing 0.2% Triton X-100 (buffer A). The Triton X-100 detergent has strong absorption in the UV region, because of the involvement of its phenyl residue. Therefore, for CD measurements, we employed Brij 35 ($C_{12}E_{23}$) as an alternative detergent, instead of Triton X-100. When dissolved in buffer B [10 mM sodium phosphate (pH 6.0) containing 0.6% Brij 35], the wild-type SHC was found to have equivalent activity (115%) to that in buffer A. The SHCs solution purified by a Ni agarose column was applied to a DEAE-Toyopearl 650 M column (Tohso), which had been previously equilibrated with buffer B. The wild-type and mutated SHCs were homogeneously purified through two steps of DEAE column chromatography; the enriched fraction of the SHCs, which had been prepared by the first chromatography with a linear gradient of a 10−50 mM sodium citrate buffer (pH 6.0) containing 0.6% Brij 35, was applied again to the column by eluting with a linear gradient of 0−0.3

M NaCl in buffer B to obtain the pure SHCs. The purity was checked by SDS-PAGE. The CD spectrum of the purified enzyme (80−100 μg/mL) in buffer B was measured at a wavelength between 200 and 250 nm across a 1-mm light path at 20−70 °C by using a JASCO J-725 instrument.

Supporting Information Available: Amino acid alignment of the wild-type and the mutated SHCs having unnatural amino acids, some additional MS data after tryptic digestion, and CD spectra measured at 20−70 °C. This material is available free of charge via the Internet at http://pub.acs.org

JA063358P